Mullite–zirconia composite for the bonding phase of refractory bricks in hazardous waste incineration rotary kiln

Adrian Villalba Weinberg, Dominique Goeuriot, Jacques Poirier, Cyrille Varona, Xavier Chaucherie

Mullite–zirconia composite for the bonding phase of refractory bricks in hazardous waste incineration rotary kiln

Adrian Villalba Weinberg[a,b,c], Dominique Goeuriot[a], Jacques Poirier[b,*], Cyrille Varona[c], Xavier Chaucherie[d]

[a] Laboratoire Georges Friedel, CNRS UMR 5307, MINES Saint-Étienne, 158 Cours Fauriel, 42023 Saint-Étienne, France
[b] Conditions Extrêmes et Matériaux: Haute Température et Irradiation (CEMHTI), CNRS UPR 3079, Université d'Orléans, 1D Avenue de la Recherche Scientifique, 45071 Orléans, France
[c] BONY SA – Produits Réfractaires, 53 Boulevard Fauriat, 42001 Saint-Étienne, France
[d] SARPI-VEOLIA, 427 Route du Hazay, 78520 Limay, France

*Corresponding Author. E-mail: jacques.poirier@univ-orleans.fr; Tel.: +33 (0) 238 25 55 14; Fax: +33 (0) 238 63 81 03.

Abstract

Although mullite–zirconia composites made from zircon, alumina, and andalusite meet the requirements for many refractory applications, little effort has been made to transfer these composites to the bonding phase (the 'matrix') of refractory bricks. In this paper, we investigate how this could be achieved through better control of secondary oxides. The high temperature phases were simulated with thermodynamic software and linked to the microstructures, mineralogy, and properties of the composites. The results revealed that the system is very sensitive to Na_2O, which harmed the microstructure considerably. By contrast, TiO_2 and P_2O_5 additions proved beneficial, allowing complete zircon decomposition at 1550 °C while providing the required green strength. Decohesion between the matrix and aggregates due to high matrix shrinkage can be prevented by partially substituting andalusite with the volume-increasing mineral kyanite. Based on these findings, a novel refractory brick was developed and tested with success at an industrial scale.

Keywords: mullite/zirconia; reaction sintering; phosphate; cyanite; microstructure

1 Introduction

Reaction-sintered mullite–zirconia ceramics that use zircon ($ZrSiO_4$) as the zirconia source have many beneficial qualities as refractory materials, including refractoriness, chemical stability in contact with slag [1], high strength [2,3], and outstanding thermal shock resistance [4,5]. These properties make mullite-zirconia a promising candidate as bonding system of novel refractories for hazardous waste incinerators, because mullite-zirconia exhibits excellent thermal shock resistance in comparison with bauxite, andalusite or alumina-chromia refractory bricks or castables used nowadays. The *in-situ* formation of 20 vol% well-dispersed zirconia grains raises the material's strength and fracture toughness by up to 50% [2] compared to that of plain mullite. Nevertheless, these results are obtained when using high-purity ceramic powders; it is difficult to transfer them to refractory bricks, where the bonding phase (the 'matrix') is made from raw materials containing impurities.

Therefore, despite the potential advantages of using a mullite–zirconia bonding phase, most refractory bricks are still mullite-bonded.

Refractory manufacturers use graded particle size distributions, with particle sizes ranging from a few microns to a few millimetres. The finer part of this distribution (≤200 μm; typically 30–40% of the total raw material) forms the matrix; larger particles are considered aggregates. The matrix materials ought to be economically priced and accessible in large quantities.

Many studies in recent years have attempted to employ different aluminosilicates for the synthesis of mullite–zirconia composites. Minerals from the sillimanite group have attracted most attention [1,6–8]. These comprise sillimanite, andalusite, and kyanite, which are all polymorphs of Al_2SiO_5. In addition to the economic advantage, mullite-transformed andalusite can enhance the thermal shock resistance of the composite [1]. The starting materials $ZrSiO_4$, Al_2O_3, and Al_2SiO_5 react in several steps to form mullite and zirconia, which, simplified, can be summarised to reaction (1), where $0 \leq x \leq 0.667$.

$$(2-3x)Al_2SiO_5 + Al_2O_3 + xZrSiO_4 \rightarrow (1-x)Al_6Si_2O_{13} + xZrO_2 \quad (1)$$

The sintering reaction is very sensitive to the presence of secondary oxides [9], which are omnipresent in refractory-grade raw materials, either in the form of impurities or intentionally added as sintering aids, pressing aids, temporary binders, etc. In this respect, Na_2O, TiO_2, and P_2O_5 are critical. Na_2O is a major impurity in Bayer alumina. TiO_2 is a common impurity in many raw materials, but it is also a common sintering aid for mullite–zirconia composites [3,10]. P_2O_5 is a prominent additive in the refractory industry as it provides the required green strength and plasticity [11], and reacts with alumina at high temperatures to form $AlPO_4$, which reinforces the refractory bonding [12]. However, while the effects of Na_2O and TiO_2 on the sintering reaction have been studied in detail, the effect of phosphate is not well understood. Therefore, there is a need to investigate the effects of P_2O_5 additives and to compare them to the effects of Na_2O and TiO_2, for the refractories studied in this paper.

In this study, we apply a mullite–zirconia matrix made from zircon–alumina–andalusite/kyanite mixes to the bonding phase of refractory bricks and we investigate the effects of P_2O_5, Na_2O, and TiO_2 on the system. The findings offer an understanding of how to successfully control the reaction-sintering process in refractory bricks. First, we focus on the matrix itself, regarding the phases that form at high temperature. Second, we shed light on the matrix–aggregate interdependence within a refractory brick. We also address the problem of matrix shrinkage and explain how kyanite can help to solve this problem.

2 Materials and methods

2.1 Fabrication of matrix samples

Matrix samples were synthesised through a laboratory processing route that aims to reproduce the industrial process, albeit at a smaller scale. The task was to transfer the matrix, elaborated in the laboratory, to an industrial refractory brick made of matrix (bonding phase) and aggregates. The main requirements with regard to the industrial process are short and dry mixing, uniaxial pressing, and sintering below 1600 °C.

Matrix samples were prepared by mixing the raw materials in a tumbler mixer (Turbula® T2C) for 2 h. The absence of aggregates was compensated by adding alumina balls (Ø10 mm) to aid the mixing process, which were subsequently removed. The blended mixture was then pressed into pills (Ø20 × 10 mm) using a uniaxial

pressure of 150 MPa (5584, Instron, US). The matrix pills were sintered at various temperatures between 1450 and 1600 °C. The heating and cooling rates were 2.5 °C/min and the holding time was 3 h.

Preliminary tests showed that using only very fine powders led to agglomeration during mixing and lamination during pressing. Both problems were resolved by designing a graded particle size distribution with fine zircon powder, intermediate alumina, and coarser andalusite or kyanite (Table 1). A portion of the andalusite was replaced with kyanite (percentage *k* in table 1) to mitigate matrix shrinkage (see Section 3.2).

Table 1. Raw material composition for matrix (without additives) and aggregate materials.

	Grain size	Composition [wt%]										wt% of
Matrix component	**[µm]**	**Al_2O_3**	**SiO_2**	**Fe_2O_3**	**TiO_2**	**P_2O_5**	**Na_2O**	**K_2O**	**CaO**	**MgO**	**ZrO_2**	**matrix**
Micronized zircon	≈2	0.7	34.0	0.10	0.25	0.12	0.00	0.00	0.00	0.20	64.0[3]	31.3
Calcined alumina	≈4	99.5	0.0	0.01	0.00	0.00	0.27	0.00	0.01	0.00	0.0	22.9
Fused alumina	≈50	99.7	0.0	0.02	0.00	0.00	0.16	0.00	0.01	0.01	0.0	15.2
Andalusite	<160	60.8	38.1	0.50	0.15	0.00	0.10	0.15	0.05	0.10	0.0	30.6-*k*
Kyanite	<125	57.5	40.3	0.6	1.2	0.15	0.04	0.07	0.04	0.03	–	*k*
Matrix	2–160	56.8	22.3	0.19	0.12	0.04	0.12	0.05	0.02	0.09	20.0[3]	100.0
Aggregate												
Andalusite	100–1600	58.7	38.5	1.1	0.2	–	0.1	0.4	0.2	0.2	–	
Mulcoa 60[1]	1000–6000	60.0	35.8	1.2	2.4	–	0.1	0.1	0.1	0.1	–	
FZM[2]	100–6000	45.8	17.1	0.1	0.1	–	–	–	0.1	–	36.5[3]	

[1]High alumina chamotte; [2]Fused zirconia–mullite; [3]ZrO_2+HfO_2

To analyse the effects of Na_2O, TiO_2, and P_2O_5 oxide additions on the matrix properties and sintering reactions, fine powders of Na_2CO_3, rutile (TiO_2), and monoaluminum phosphate ($Al(H_2PO_4)_3$) were respectively added to the raw materials, to give an equivalent oxide content of 1, 2, or 3 mol%.

2.2 Fabrication of brick samples

Brick samples (Wedges of 250 × 198 × 103/90 mm) were prepared by mixing the starting materials (aggregates, matrix components, water) in an Eirich-type mixer. The aggregate/matrix volume ratio was 7:3 for all samples. The amount of water was adjusted to yield 2 wt% moisture in every blend. The grain size distribution was designed following the modified Andreasen model developed by Dinger and Funk [13]. The maximum and minimum grain sizes of 6 mm and 2 µm, respectively, were the same for all formulations. After a total mixing time of 30 min, the batch was pressed to bricks using a uniaxial pressure of 150 MPa. Finally, the bricks were dried overnight at 110 °C and fired at 1500, 1550, or 1600 °C. The heating rate and dwell time were the same as for the sintering step of the matrix samples (2.5 °C/min and 3 h, respectively).

The brick formulations contained the same matrix, composed of 31.3 wt% zircon, 37.8 wt% alumina, 10.2 wt% andalusite, 15 wt% kyanite, 2.6 wt% (3 mol%) TiO_2, and 3.1 wt% (2 mol%) P_2O_5. Various aggregate systems were evaluated, but only the two most suitable systems are presented in this paper. The first system used a combination of andalusite (0.1–1.6 mm) and high alumina chamotte (1–6 mm) aggregates, while the second system used fused zirconia–mullite (FZM; 0.1–6 mm) aggregates. The chemical compositions of the studied aggregates are summarised in Table 1.

2.3 Thermodynamic modelling

The equilibrium phases at 1000–1600 °C were calculated using FactSage® (version 6.4), a thermodynamic database computing software. The FactPS and FToxid databases (both updated in 2013) were used for pure substances and oxides, respectively. The ambient pressure was set to 1 atm. Due to missing/erroneous data of K_2O compounds, the percentage of K_2O was added to the Na_2O content; since these alkali oxides are chemically alike, this should not considerably distort the resulting liquid portion.

2.4 Characterisation methods

The microstructures, mineral compositions, and properties (porosity, compressive strength) of the sintered samples were evaluated with regard to the thermodynamic calculation results. The microstructures were examined using scanning electron microscopy (SEM; JSM-6500F, JEOL, Japan) with polished and carbon-metallised samples. For better contrast between zircon, zirconia, and mullite, the backscattering mode was chosen. The crystalline phases in the matrix were determined for the matrix pills by X-ray diffraction (PANalytical X'Pert Pro, Netherlands) using Cu Kα radiation. The open porosity was measured via Archimedes' method according to DIN EN 993-1. The cold crushing strength (CCS) of the refractories was measured according to DIN EN 993-5 on cubes of 50 × 50 × 50 mm.

3 Results

3.1 Effects of secondary oxides on mineralogy and microstructure

The diffraction patterns in Fig. 1 of zircon–alumina–andalusite mixtures (without additives) sintered at different temperatures demonstrate that zircon dissociation actually takes place between 1450 and 1570 °C.

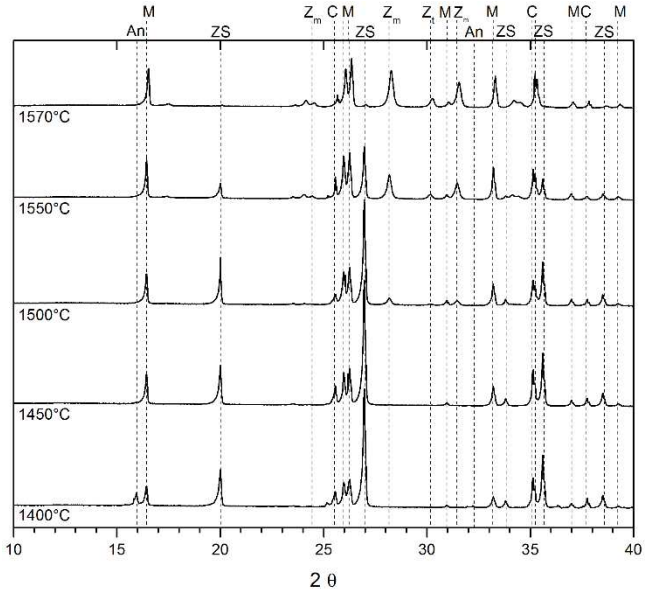

Fig. 1. X-ray diffraction patterns of a zircon–alumina–andalusite mixture (without additives) sintered at different temperatures. The mineralogical phases are C – corundum (Al_2O_3), M – mullite ($Al_6Si_2O_{13}$), An – andalusite (Al_2SiO_5), ZS – zircon ($ZrSiO_4$), Z_m – monoclinic zirconia (m-ZrO_2), and Z_t – tetragonal zirconia (t-ZrO_2).

The effects of secondary oxides are illustrated in the diffractograms in Fig. 2. Adding 1 mol% (0.34 wt%) Na_2O lowers the zircon transformation start and finish temperatures by approximately 50 °C. By 1500 °C,

almost all the zircon has already dissociated. The obtained zirconia particles comprise tetragonal and monoclinic modifications.

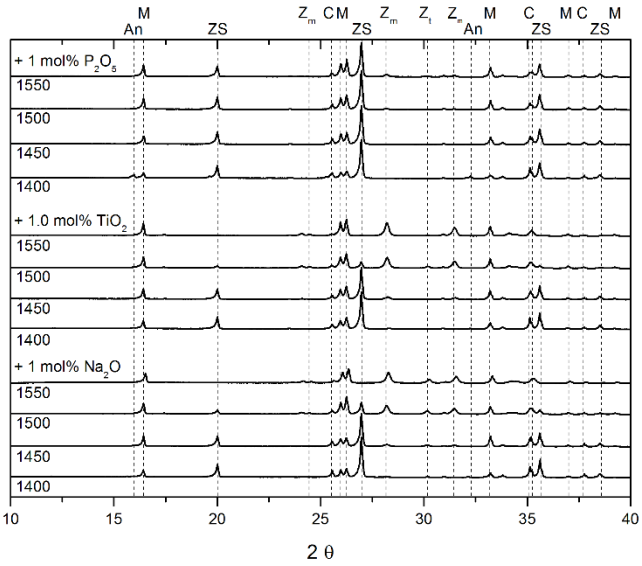

Fig. 2. X-ray diffraction patterns of zircon–alumina–andalusite–additive mixtures sintered at different temperatures. The mineralogical phases are C – corundum (Al_2O_3), M – mullite ($Al_6Si_2O_{13}$), An – andalusite (Al_2SiO_5), ZS – zircon ($ZrSiO_4$), Z_m – monoclinic zirconia (m-ZrO_2), and Z_t – tetragonal zirconia (t-ZrO_2).

Among the three investigated oxides, TiO_2 is the most effective at promoting zircon dissociation. The zircon peaks have mostly disappeared in the diffractogram of the sample fired at 1500 °C, whereas the zircon peaks are still well pronounced in the Na_2O-doped sample sintered at the same temperature. Tetragonal zirconia was not detected in any of the TiO_2-doped samples.

For the P_2O_5-doped samples, the X-ray survey testifies a slight shift of both andalusite and zircon dissociation towards higher temperatures. After sintering at 1550°C, the zircon peaks are yet well visible on the diffractogram. Contrary to our expectations, crystalline $AlPO_4$ was not detected by X-ray diffraction. $AlPO_4$ might have been incorporated into the silica-rich amorphous phase, considering that $AlPO_4$ and SiO_2 are chemically similar [14]. To verify this, a silica-free matrix was fabricated from alumina, zirconia, and $Al(H_2PO_4)_3$. X-ray diffraction measurements confirmed that in this case, crystalline $AlPO_4$ is indeed formed. Therefore, when in contact with the silica-rich amorphous phase present in the mullite–zirconia composites, phosphate is likely to form an amorphous phase instead of crystalline $AlPO_4$.

In order to observe how zircon starts to dissociate, the same area of an additive-free matrix sample was imaged sequentially after heating to 1450 and 1475 °C. The SEM images in Fig. 3 show two newly formed zirconia grains after the second heating step, which emerged from several adjacent zircon particles. Meanwhile, non-transformed zircon particle clusters did not coalesce.

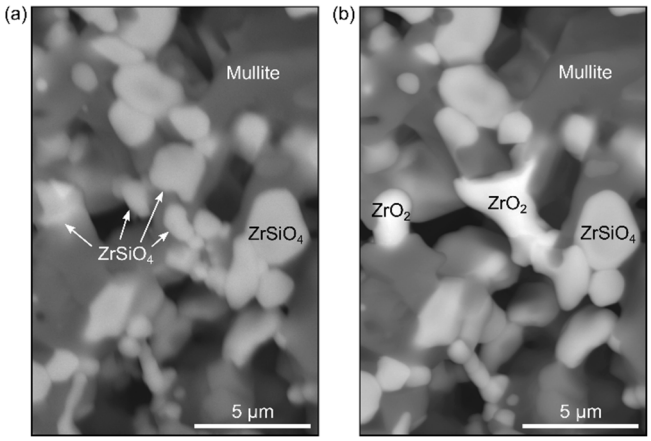

Fig. 3. SEM images of a zircon–alumina–andalusite matrix sample (without additives) after heat treatments at (a) 1450 °C and (b) 1475 °C.

The effects of the three additives on the microstructures can be compared in Fig. 4. When Na_2O is added (Fig. 4 (b)), the resulting ZrO_2 particles are 0.5–3 µm in size, which is noticeably smaller than those in the other samples. However, there are notable amounts of amorphous phase. The liquid phase causes densification of the matrix sample, leading to reduced porosity.

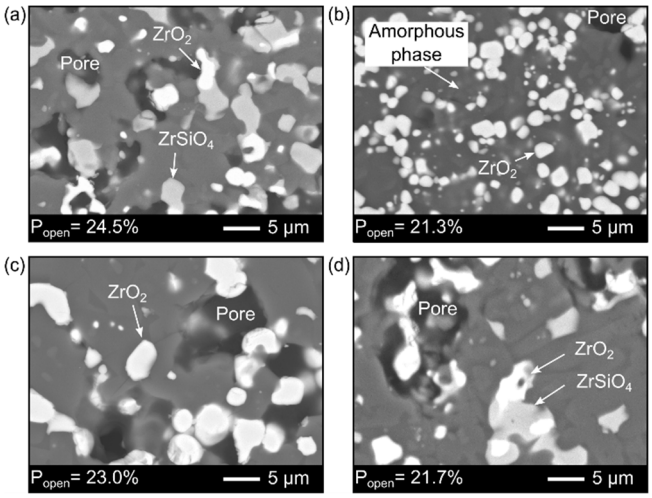

Fig. 4. SEM images showing the impact of additives (1 mol%) on the final microstructure and open porosity (P_{open}) of zircon–alumina–andalusite mixtures sintered at 1550 °C: (a) without additives, (b) 0.34 wt% Na_2O, (c) 0.88 wt% TiO_2, and (d) 1.55 wt% P_2O_5.

With the addition of TiO_2 (Fig. 4 (c)), zircon is completely transformed after sintering at 1550 °C. Nevertheless, the microstructure does not vitrify, contrary to the case for Na_2O, although the porosity is still reduced somewhat compared to that in the additive-free matrix. The final zirconia grains are about 5 µm in size, similarly to the zirconia grains in the additive-free matrix with fully dissociated zircon (sintered at 1570 °C).

The impact of P_2O_5 on the zircon decomposition is marginal (Fig. 4 (d)). The morphology is similar to that of the additive-free matrix, with some zircon particles still remaining after sintering at 1550 °C. However, the porosity is reduced on account of the improved compaction during pressing.

Further experiments revealed that a combination of 2 mol% P_2O_5 and 3 mol% TiO_2 provided optimal green properties and complete zircon dissociation at 1550 °C. Therefore, these combined additives were chosen for the brick samples.

3.2 The preparation of bricks

During the development of the bricks, there was a noticeable drop in mechanical strength when a certain sintering temperature was surpassed. SEM observations revealed that this was caused by high shrinkage of the matrix, as it let to decohesion between the aggregates and matrix. An example is illustrated in Fig. 5.

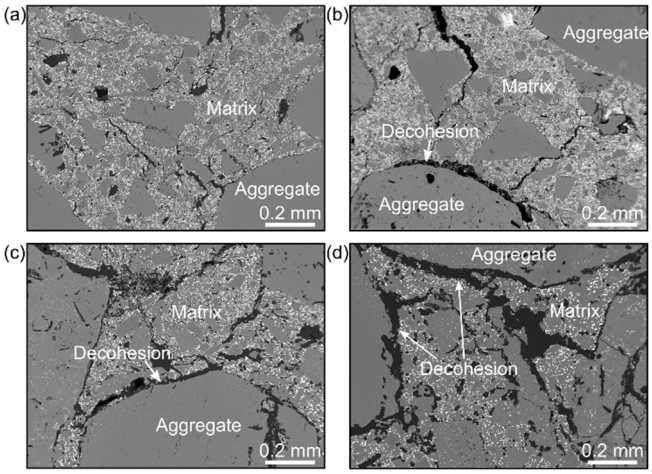

Fig. 5. SEM images of a mullite–zirconia-bonded brick sintered at (a) 1450 °C, (b) 1500 °C, (c) 1550 °C, and (d) 1600 °C, revealing decohesion between the matrix and aggregates (Mulcoa 60) caused by matrix shrinkage.

It is possible to counter high matrix shrinkage by employing materials that increase in volume during sintering. Kyanite (Al_2SiO_5), a polymorph of andalusite, has such an effect. Thus, to counterbalance the shrinkage, the andalusite in the matrix was gradually replaced by kyanite. Fig. 6 shows that, in the additive-free matrix, approximately one third of the andalusite needs to be replaced by kyanite to obtain a matrix that neither shrinks nor expands at 1550 °C. Accordingly, the kyanite and andalusite contents of the matrix were adjusted to attain zero shrinkage when sintering at 1550 °C.

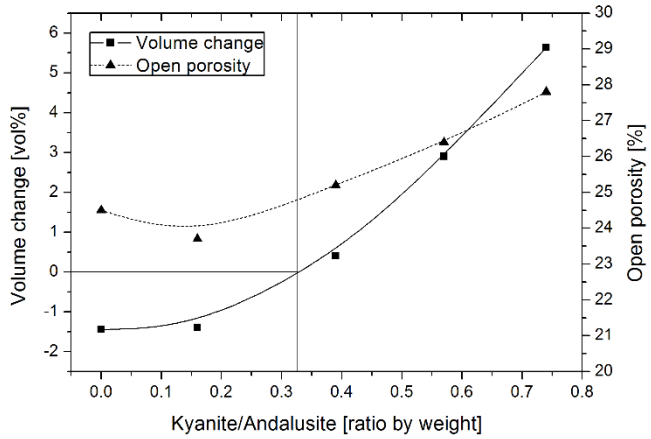

Fig. 6. Impact of kyanite on the volume expansion and porosity of a reaction-sintered (1550 °C) mullite–zirconia (20 wt% ZrO_2) matrix made from andalusite/kyanite, alumina, and zircon (without additives).

Representative microstructures of the bricks with andalusite/Mulcoa 60 and FZM aggregates are depicted in Fig. 7 (a) and (b), respectively. In both cases, the zirconia particles are well distributed and there are no large gaps between the aggregates and matrix. However, fine cracks appeared at the matrix/aggregate interface when using andalusite/Mulcoa 60 aggregates, which were absent when using the FZM aggregates.

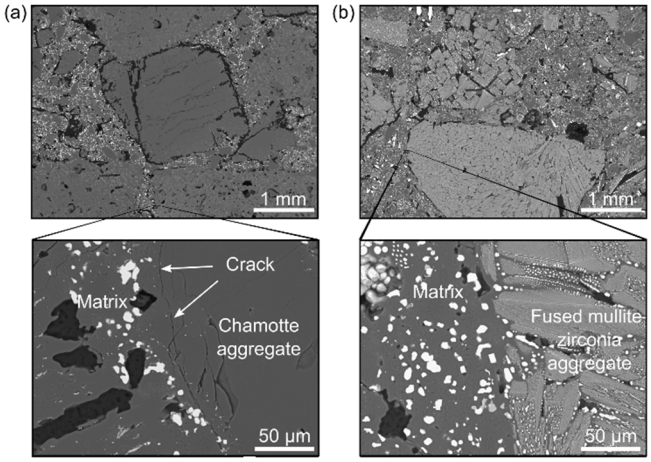

Fig. 7. SEM images of mullite–zirconia-bonded refractory bricks made with (a) andalusite/Mulcoa 60 aggregates and (b) fused zirconia–mullite aggregates (FZM). Both bricks used the same matrix (31.3 wt% zircon, 37.8 wt% alumina, 10.2 wt% andalusite, 15 wt% kyanite, 2.6 wt% (3 mol%) TiO_2, and 3.1 wt% (2 mol%) P_2O_5) and sintering temperature (1550 °C).

3.3 Properties of novel bricks and applications

The sintering temperature had a clear impact on the mechanical properties of the bricks (Fig. 8). Because the andalusite/kyanite ratio and additive content were respectively designed to give zero matrix shrinkage and complete zircon dissociation at 1550 °C, a maximum in strength was obtained when sintering at 1550 °C. If the sintering temperature is above or below this designed temperature, the desired matrix properties are no longer guaranteed.

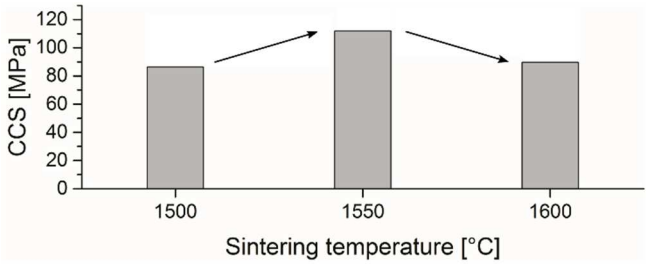

Fig. 8. Cold crushing strength (CSS) vs. sintering temperature of a mullite–zirconia-bonded brick (Aggregates: andalusite/Mulcoa 60).

Fig. 9 compares the properties of bricks sintered at 1550 °C with and without P_2O_5 in the matrix. The phosphate addition lowered the porosity and greatly increased the strength. This effect was even more pronounced for the brick with FZM aggregates, because the phosphate bonds between the aggregates and matrix are intact (see Fig. 7). The typical compressive strengths obtained with FZM aggregates and P_2O_5 doping were >200 MPa, which is exceptional for refractory bricks.

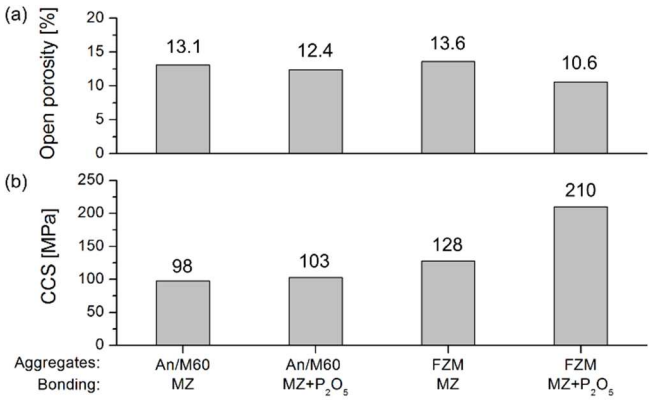

Fig. 9. Comparison of (a) open porosity and (b) cold crushing strength (CSS) of mullite–zirconia (MZ)-bonded bricks with and without 2 mol% P_2O_5 in the matrix. Andalusite/Mulcoa 60 (An/M60) and fused zirconia–mullite (FZM) aggregates were used. All bricks were sintered at 1550 °C.

The mullite–zirconia-bonded brick with FZM aggregates was produced industrially and tested in two rotary kilns for hazardous waste incineration. The material had very good performance in the kiln inlet, where the refractory bricks were exposed to mechanical load caused by solid wastes and to thermal shock provoked by cold liquid wastes dropping on the hot refractory lining [15]. After 20 months of use, the lining thickness was reduced in the first kiln from 250 to 180 mm and in the second kiln from 250 to 200 mm. With these slow wear rates, a lifetime of five to seven years is expected to be attained, in comparison to only one to two years for the previously used bauxite, andalusite, and alumina–chromia refractory bricks or castables.

4 Discussion

Prior studies have showcased the benefits of mullite–zirconia composites made from zircon, alumina, and andalusite. In this study, we investigated the possibility of applying this material as the bonding matrix phase of refractory bricks, with a focus on the impacts of secondary oxides on the high temperature sintering reactions, microstructure, and resulting properties.

The sintering process of $ZrSiO_4$–Al_2O_3–Al_2SiO_5 mixtures can be divided into four steps, represented by Reactions (2)–(5).

$$3\underbrace{Al_2SiO_5}_{\substack{\text{Sillimanite,}\\ \text{andalusite,}\\ \text{or kyanite}}} \rightarrow \underbrace{Al_6Si_2O_{13}}_{\substack{\text{Mullite-transformed}\\ \text{sillimanite,}\\ \text{andalusite,or kyanite}}} + SiO_2 \quad (2)$$

$$2SiO_2 + 3Al_2O_3 \rightarrow \underbrace{Al_6Si_2O_{13}}_{\text{Primary mullite}} \quad (3)$$

$$ZrSiO_4 \rightarrow ZrO_2 + SiO_2 \quad (4)$$

$$2SiO_2 + 3Al_2O_3 \rightarrow \underbrace{Al_6Si_2O_{13}}_{\text{Secondary mullite}} \quad (5)$$

The first two mullitisation steps (Reactions (2) and (3)) begin at about 1300 °C upon heating and conclude at around 1400 °C [1,16]. From a technological point of view, the critical step is zircon decomposition (Reaction (4)), because it requires a high temperature. Pure zircon dissociates into zirconia and silica at 1673 °C [17]. In the presence of alumina, this temperature reduces to 1450–1600 °C, depending on the reactivity and purity of

the starting powders [9,18,19]. The last step (Reaction (5)) is the reaction between the zircon-released silica and the remaining alumina to form secondary mullite.

4.1 Role of impurities and alkaline/TiO_2 sintering aids

All four reactions (2) – (5) are diffusion dependent, making them sensitive to the presence of a liquid phase. This explains why impurities, in particular fluxing agents, are so critical to this system – in both a positive and negative sense [9]. On one hand, they accelerate the reaction sintering processes, but on the other, they can harm the microstructure and deteriorate the final properties.

The thermodynamically stable phases of a theoretical 30% $ZrSiO_4$–36% Al_2O_3–34% Al_2SiO_5 (wt%) mixture without impurities and those of the same mixture including impurities (0.17 wt% Na_2O, 0.12 wt% TiO_2, 0.19 wt% Fe_2O_3, 0.09 wt% MgO, and 0.02 wt% CaO) are shown in Fig. 10(a) and (b), respectively. In the theoretical composition without impurities, insignificant amounts (0.2 wt%) of liquid phase appear at 1556 °C. However, when the impurities are considered, a liquid phase emerges at only 1074 °C. This phase contains some SiO_2 and Al_2O_3 and all the accessible Na_2O. By 1200 °C, the liquid phase comprises 1.3 wt% of the matrix. At 1300 °C and above, MgO, CaO, and Fe_2O_3 enter the liquid state and increasing amounts of SiO_2, Al_2O_3, and some ZrO_2 dissolve. At 1550 °C, 3.0 wt% liquid is formed. Moreover, between 1300 and 1600 °C, mullite transforms from $3Al_2O_3{\cdot}2SiO_2$ (3:2 mullite) to $2Al_2O_3{\cdot}SiO_2$ (2:1 mullite). This transformation is possibly related to the liquid phase, as it does not occur in the impurity-free calculation. It should be noted that zirconia is thermodynamically preferred over zircon ($ZrSiO_4$) at 1008 °C. However, from a kinetic point of view, this temperature is too low for the diffusion processes, so zircon does not actually decompose at this low temperature. This also implies that ZrO_2 does not transform back into $ZrSiO_4$ during cooling.

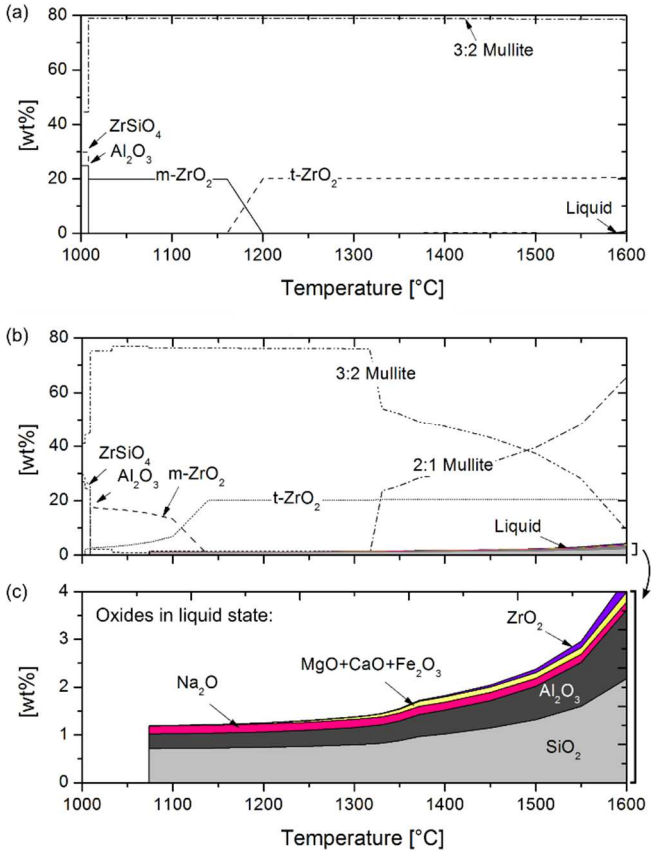

Fig. 10. Equilibrium phases of a 30% $ZrSiO_4$–36% Al_2O_3–34% Al_2SiO_5 (wt%) mixture (a) excluding and (b) including impurities (0.17 wt% Na_2O, 0.12 wt% TiO_2, 0.04 wt% P_2O_5, 0.19 wt% Fe_2O_3, 0.09 wt% MgO, and 0.02 wt% CaO). (c) Expanded view of oxides in liquid state for the impurity-containing matrix. m- and t-ZrO_2 are monoclinic and tetragonal zirconia, respectively.

These thermodynamic calculations demonstrate that even a low impurity content in the raw materials generates non-negligible amounts of liquid phase, which reduce the zircon decomposition temperature. In our experiments, the zircon decomposition had begun by 1470 °C and was completed by 1570 °C, despite the relatively coarse-grained raw materials.

The effects of secondary oxide additions (Na_2O, TiO_2, and P_2O_5) are exhibited in the equilibrium phase diagrams in Fig. 11. The Na_2O addition had a strong but negative impact. According to the thermodynamic calculations depicted in Fig. 11(a), an addition of 0.3 wt% Na_2O would triple the liquid portion at 1200 °C (from 1.3 to 3.8 wt%) and more than double it at 1550 °C (from 3.0 to 6.6 wt%). Consequently, Na_2O shifted the first two mullitisation steps to lower temperatures. This might explain the smaller zirconia grain sizes obtained when Na_2O was added: the low temperature liquid could have promoted primary mullite growth (Reaction (3)), and the zirconia grains from zircon decomposition could have been trapped within the primary mullite network, hindering the zirconia grains from growing together. Unfortunately, while the small grain size is desirable, the final matrix exhibited very high amounts of a glassy phase. Thus, Na_2O is highly undesirable for refractory purposes.

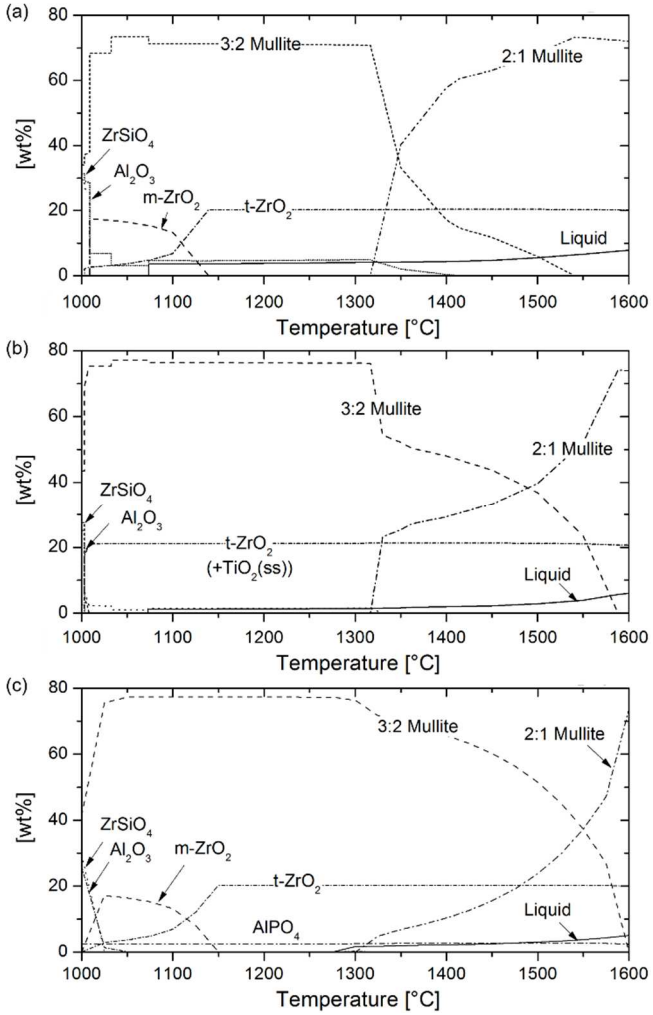

Fig. 11. Impacts of 1 mol% oxide additions on the thermodynamic equilibrium of a 30% $ZrSiO_4$–36% Al_2O_3–34% Al_2SiO_5 (wt%) mixture (including impurities): (a) +0.34 wt% Na_2O, (b) +0.88 wt% TiO_2, and (c) +1.55 wt% P_2O_5. m- and t-ZrO_2 are monoclinic and tetragonal zirconia, respectively. ss: solid solution.

The TiO_2 addition showed a completely different behaviour. It effectively promoted zircon dissociation while generating minor amounts of amorphous phase (Fig. 11 (b)). The addition of 1 mol% (0.88 wt%) TiO_2 generates 1.3 and 3.9 wt% liquid at 1200 and 1550 °C, respectively, which is slightly greater than that in the additive-free matrix. Moreover, the results indicate that TiO_2 forms a solid solution with ZrO_2, which stabilises the tetragonal zirconia (t-ZrO_2) modification below 1170 °C. These results are in accordance with those of Melo et al. [20], who emphasised that TiO_2 forms a transitory liquid phase at about 1400 °C and then diffuses into the ZrO_2 and mullite crystals, which can both accommodate 4 wt% TiO_2. Nevertheless, the stabilising effect of TiO_2 on the t-ZrO_2 phase suggested in the literature and our thermodynamic calculations was not observed experimentally in our TiO_2-doped samples. It could be that TiO_2 merely did not have enough time to diffuse from the transitory liquid phase into the zirconia grains. Furthermore, the rather high zirconia grain size (5 µm) and the high porosity both work against the tetragonal zirconia stabilisation. Nonetheless, zirconia stabilisation is a rather unimportant detail for refractory materials, because their operating temperatures are usually above the m↔t transformation temperature. Overall, TiO_2 is a suitable sintering aid for mullite–zirconia-bonded refractory materials.

4.2 Role of phosphate

In mullite-bonded bricks, plasticity and green strength are provided by clay. However, owing to the high silica content of clay, it can only be used in reaction-sintered mullite–zirconia at the expense of reducing the zircon content or by accepting a portion of free silica in the sintered matrix. P_2O_5 precursors represent a more suitable alternative to clay. Just a few percent of a viscous monoaluminum phosphate solution assures sufficient green strength by delivering the required plasticity and forming chemical bonds at ambient temperature [11]. At high temperatures, $AlPO_4$ is formed [12], which can reinforce the mullite–zirconia bonding.

In the investigated materials, P_2O_5 considerably reduced the porosity and increased the mechanical strength owing to the improved pressing behaviour and additional (amorphous) $AlPO_4$ bonding. The impact of phosphate on the high temperature equilibrium was marginal (Fig. 11 (c)). The liquid phase accounts for 3.9 wt% of the matrix at 1550 °C, which is the same as that for the TiO_2-containing matrix, and only 0.9 wt% more than that in the additive-free mixture. However, thermodynamic modelling suggested that P_2O_5 has a slight retarding effect on the liquid phase formation. In the P_2O_5-doped mixture, the calculations predict the formation of a liquid phase at approximately 1300 °C, i.e. 200 °C higher than that for the additive-free matrix. Consequently, the primary mullitisation step and the zircon decomposition were delayed. To enable full zircon dissociation at 1550 °C, the phosphate needed to be added in conjunction with TiO_2. The matrix with 2 mol% P_2O_5 and 3 mol% TiO_2 yielded the most promising results. A patent covering this bonding phase has been applied for.

4.3 Problem of and solution for matrix shrinkage

While shrinkage does not pose a substantial problem in classic ceramics, shrinkage is undesirable in refractory matrices. This is because the coarse and dense aggregates show practically no shrinkage during sintering. In fact, they form a rigid structure of closely packed aggregates which prevent the brick from shrinking. Hence, a shrinking matrix does not pull the aggregates closer together, but instead causes decohesion between the aggregates and matrix, as illustrated by the micrographs in Fig. 5. The high shrinkage associated with reaction-sintered ceramics therefore poses a serious problem for refractory bricks.

We have demonstrated that kyanite is a well-adapted solution to this problem. Kyanite has the same chemical composition as andalusite (Al_2SiO_5) but a higher density. Upon heat treatment, both kyanite and andalusite are analogously dissociated into mullite and a silica-rich amorphous phase [21]. The volume change of this mullitisation process can be calculated from the molar volumes, specified in [22]. Assuming complete mullitisation according to Reactions (2) and (3), the resulting theoretical expansion is 18.3 vol% for kyanite, yet only 4.6 vol% for andalusite. By substituting a portion of the andalusite for kyanite, the net volume change of the matrix can be reduced to zero at a given sintering temperature. Evidently, kyanite's enormous volume change can cause cracking, cavities, and increased porosity if excessive kyanite is added; therefore, it should be dosed cautiously.

4.4 Implications for the sintering curve

By tailoring the matrix shrinkage to a specific sintering temperature, it is paramount to strictly comply with this exact temperature during fabrication. Otherwise, decohesion between the matrix and aggregates is likely to occur, weakening the material.

Slow heating and cooling rates are also suggested for the following reasons. Our SEM observations revealed that adjacent zircon particles dissociate simultaneously, and that the newly formed zirconia particles subsequently grow together. It can be deduced that the silica released upon zircon dissociation activates the

dissociation of the surrounding zircon particles and enables the coalescence of particles. This supports the theory of Di Rupo and Anseau [18]; the released silica first forms a viscous pre-mullite phase that gradually dissolves the neighbouring alumina before eventually crystallising. This viscous pre-mullite phase may enable the embedded zircon and zirconia particles to merge together, increasing the ZrO_2 grain size. On the contrary, if the primary mullite crystals are well developed before zircon starts to dissociate, they could help to inhibit coalescence. Therefore, slow heating rates or a dwell at 1400 °C should be conducted to obtain smaller ZrO_2 grains.

At high temperatures, 2:1 mullite is thermodynamically preferred over 3:2 mullite, especially when the liquid portion is high. It is likely that the 3:2 → 2:1 mullite transformation accelerates liquid formation even further because it releases free silica. In other words, the liquid itself promotes the formation of more liquid. Schmücker et al. [23] investigated the mullite transformation experimentally, and found that the liquid phase is essential to enable the diffusion of Si and O out of the mullite crystal and Al from the surrounding alumina particles into the 2:1-mullite crystal. Conversely, this suggests that a slow cooling rate or even a dwell at 1300 °C is preferred to give the diffusion-controlled back reaction from 2:1 → 3:2 mullite time to occur, which would reduce the amount of glassy phase in the final composite.

4.5 Aggregate choice

To successfully transfer the good matrix properties to the brick, the choice of aggregate is important. Mulcoa 60 (high alumina chamotte) had a loose interface with the matrix and therefore bestowed relatively poor strength. The loose bonding probably had two origins. First, there is a thermal expansion mismatch between the matrix and chamotte, which provoked cracking. Second, the TiO_2 impurities in Mulcoa 60 caused higher matrix shrinkage. In contrast, FZM aggregates suited well; the chemical similarity of the matrix and aggregate materials led to strong cohesion at the matrix/aggregate interface.

5 Conclusions

(1) Effects of additives and secondary phases

Phosphate precursors provide the necessary green strength and plasticity to the raw material mix. Moreover, although P_2O_5 slightly retards the zircon decomposition temperature, it effectively reduces the porosity and increases the final strength. TiO_2 is well-adapted to stimulate zircon decomposition in refractory materials, as it does not create much liquid at high temperatures. Na_2O has a highly undesirable effect on the sintering reaction because it produces excessive amounts of liquid phase at relatively low temperatures – this is even true for contents as low as 0.3 wt% Na_2O. Therefore, the raw materials must be selected carefully with respect to alkali oxides.

(2) Preparation of bricks

Matrix shrinkage should be avoided because it leads to decohesion at the matrix/aggregate interface. Partially replacing andalusite with kyanite helps to reduce the net matrix shrinkage to zero. FZM aggregates are well-suited for use with a mullite–zirconia matrix, whereas high alumina chamotte and coarse andalusite aggregates lead to cracking at the matrix/aggregate interface.

The understanding of the high temperature phase transformations suggests to apply low heating and cooling rates, for the following reasons. Slow heating rates, or a dwell at 1400 °C, should help to develop primary mullite crystals before zircon decomposition. A well-developed primary mullite network may inhibit

zirconia coalescence and eventually reduce the zirconia grain size. Slow cooling rates or, if possible, a dwell at 1300 °C are recommended to encourage the 3:2 → 2:1 mullite transformation and reduce the amorphous phase fraction.

(3) Applications

A novel mullite–zirconia-bonded refractory material has been produced and field-tested in a rotary kiln incinerator, where the material was exposed to thermal shock and mechanical load. The material persisted much longer than mullite- and alumina–chromia-bonded refractories. We believe similar success could be achieved in other refractory areas, especially if alternative and more cost-effective aggregates could be found that are compatible with this matrix.

Acknowledgements and Support

This research was realised within a PhD thesis defended on April 2017 in Saint-Étienne, France. The thesis was financed by BONY SA and the French National Association for Research and Technology (ANRT). Industrial tests were conducted in two hazardous waste incineration plants operated by SARPI-VEOLIA.

6 Literature

[1] M.L. Bouchetou, J. Poirier, L. Arbelaez Morales, T. Chotard, O. Joubert, M. Weissenbacher, Synthesis of an innovative zirconia-mullite raw material sintered from andalusite and zircon precursors and an evaluation of its corrosion and thermal shock performance, Ceram. Int. 45 (2019) 12832–12844. https://doi.org/10.1016/j.ceramint.2019.03.206.

[2] P. Boch, J.P. Giry, Preparation and properties of reaction-sintered mullite-ZrO2 ceramics, Mater. Sci. Eng. 71 (1985) 39–48. https://doi.org/10.1016/0025-5416(85)90204-6.

[3] P. Barfi Sistani, S. Mollazadeh Beidokhti, A. Kiani-Rashid, Improving the microstructural and mechanical properties of in-situ zirconia-mullite composites by optimizing the simultaneous effect of mechanical activation and additives, Ceram. Int. 46 (2020) 1472–1486. https://doi.org/10.1016/j.ceramint.2019.09.113.

[4] N.M. Rendtorff, L.B. Garrido, E.F. Aglietti, Thermal shock behavior of dense mullite–zirconia composites obtained by two processing routes, Ceram. Int. 34 (2008) 2017–2024. https://doi.org/10.1016/j.ceramint.2007.07.035.

[5] M. Hamidouche, N. Bouaouadja, H. Osmani, R. Torrecillias, G. Fantozzi, Thermomechanical behaviour of mullite-zirconia composite, J. Eur. Ceram. Soc. 16 (1996) 441–445. https://doi.org/10.1016/0955-2219(95)00110-7.

[6] P. Kumar, M. Nath, A. Ghosh, H.S. Tripathi, Synthesis and characterization of mullite–zirconia composites by reaction sintering of zircon flour and sillimanite beach sand, Bull. Mater. Sci. 38 (2015) 1539–1544. https://doi.org/10.1007/s12034-015-0890-3.

[7] H. Majidian, L. Nikzad, H. Eslami-Shahed, T. Ebadzadeh, Phase evolution, microstructure, and mechanical properties of alumina–mullite–zirconia composites prepared by iranian andalusite, Int. J. Appl. Ceram. Technol. 13 (2016) 1024–1032. https://doi.org/10.1111/ijac.12582.

[8] T. Chotard, L. Arbelaez Morales, M.-L. Bouchetou, J. Poirier, Thermomechanical characterisation of mullite zirconia composites sintered from andalusite for high temperature applications, MDPI Ceram. 2 (2019) 587–601. https://doi.org/10.3390/ceramics2040046.

[9] P. Pena, S. De Aza, The zircon thermal behaviour: effect of impurities, J. Mater. Sci. 19 (1984) 135–142. https://doi.org/10.1007/BF00553002.

[10] M.F. Melo, J.S. Moya, P. Pena, S. De Aza, Multicomponent toughened ceramic materials obtained by reaction sintering, Part 3 System ZrO2-Al2O3-SiO2-TiO2, J. Mater. Sci. 20 (1985) 2711–2718. https://doi.org/10.1007/BF00553032.

[11] W.D. Kingery, Fundamental study of phosphate bonding in refractories: II, Cold setting properties, J. Am. Ceram. Soc. 33 (1950) 242–247. https://doi.org/10.1111/j.1151-2916.1950.tb14172.x.

[12] C. Toy, O.J. Whittemore, Phosphate bonding with several calcined aluminas, Ceram. Int. 15 (1989) 167–171. https://doi.org/10.1016/0272-8842(89)90012-6.

[13] D.R. Dinger, J.E. Funk, Particle-Packing Phenomena and Their Application in Materials Processing, MRS Bull. 22 (1997) 19–23. https://doi.org/10.1557/S0883769400034692.

[14] M. Handke, M. Rokita, W. Mozgawa, Spectroscopic studies of SiO2–AlPO4 solid solutions, Vib. Spectrosc. 19 (1999) 419–423. https://doi.org/10.1016/S0924-2031(98)00083-6.

[15] A. Villalba Weinberg, C. Varona, X. Chaucherie, D. Goeuriot, J. Poirier, Extending refractory lifetime in rotary kilns for hazardous waste incineration, Ceram. Int. 42 (2016) 17626–17634. https://doi.org/10.1016/j.ceramint.2016.08.078.

[16] M.-L. Bouchetou, J.-P. Ildefonse, J. Poirier, P. Daniellou, Mullite grown from fired andalusite grains: the role of impurities and of the high temperature liquid phase on the kinetics of mullitization and consequences on thermal shocks resistance, Ceram. Int. 31 (2005) 999–1005. https://doi.org/10.1016/j.ceramint.2004.10.015.

[17] A. Kaiser, M. Lobert, R. Telle, Thermal stability of zircon (ZrSiO4), J. Eur. Ceram. Soc. 28 (2008) 2199–2211. https://doi.org/10.1016/j.jeurceramsoc.2007.12.040.

[18] E. Di Rupo, M.R. Anseau, Solid state reactions in the ZrO2 · SiO2 - αAl2O3 system, J. Mater. Sci. 15 (1980) 114–118. https://doi.org/10.1007/BF00552434.

[19] S. Lathabai, D.G. Hay, F. Wagner, N. Claussen, Reaction-Bonded Mullite/Zirconia Composites, J. Am. Ceram. Soc. 79 (1996) 248–256. https://doi.org/10.1111/j.1151-2916.1996.tb07905.x.

[20] J.S. Moya, M.I. Osendi, Microstructure and mechanical properties of mullite/ZrO2 composites, J. Mater. Sci. 19 (1984) 2909–2914. https://doi.org/10.1007/BF01026966.

[21] J.W. Creig, Formation of mullite from Cyanite, Andalusite, and Sillimanite, J. Am. Ceram. Soc. 8 (1925) 465–484. https://doi.org/10.1111/j.1151-2916.1925.tb16771.x.

[22] R.A. Robie, K.M. Beardsley, P.M. Bethke, Selected X-ray crystallographic data, molar volumes and densities of minerals and related substances, U.S. Government Printing Office, 1967.

[23] M. Schmücker, B. Hildmann, H. Schneider, Mechanism of 2/1- to 3/2-mullite transformation at 1650 °C, Am. Mineral. 87 (2002) 1190–1193. https://doi.org/10.2138/am-2002-8-918.